Compromised mutant EFEMP1 secretion associated with macular dystrophy remedied by proteostasis network alteration

John D. Hulleman[a,b], Shalesh Kaushal[c], William E. Balch[b,d], and Jeffery W. Kelly[a,b]
[a]Departments of Chemistry and Molecular and Experimental Medicine and [b]Skaggs Institute for Chemical Biology, Scripps Research Institute, La Jolla, CA 92037; [c]Department of Ophthalmology, University of Massachusetts Medical School, Worcester, MA 01655; [d]Departments of Cell Biology and Chemical Physiology, Scripps Research Institute, La Jolla, CA 92037

ABSTRACT **An Arg345Trp (R345W) mutation in epidermal growth factor–containing, fibulin-like extracellular matrix protein 1 (EFEMP1) causes its inefficient secretion and the macular dystrophy malattia leventinese/Doyne honeycomb retinal dystrophy (ML/DHRD). To understand the influence of the protein homeostasis (or proteostasis) network in rescuing mutant EFEMP1 misfolding and inefficient secretion linked to ML/DHRD, we developed a convenient and sensitive cell-based luminescence assay to monitor secretion versus intracellular accumulation. Fusing EFEMP1 to *Gaussia* luciferase faithfully recapitulates mutant EFEMP1 secretion defects observed previously using more cumbersome methodology. To understand what governs mutant intracellular retention, we generated a series of R345 mutants. These mutants revealed that aromatic residue substitutions (i.e., Trp, Tyr, and Phe) at position 345 cause significant EFEMP1 secretion deficiencies. These secretion defects appear to be caused, in part, by reduced native disulfide bonding in domain 6 harboring the 345 position. Finally, we demonstrate that mutant EFEMP1 secretion and proper disulfide formation are enhanced by adaptation of the cellular environment by a reduced growth temperature and/or translational attenuation. This study highlights the mechanisms underlying the inefficient secretion of R345W EFEMP1 and demonstrates that alteration of the proteostasis network may provide a strategy to alleviate or delay the onset of this macular dystrophy.**

Monitoring Editor
Ramanujan Hegde
National Institutes of Health

Received: Aug 15, 2011
Revised: Oct 7, 2011
Accepted: Oct 19, 2011

INTRODUCTION

Age-related macular degeneration (AMD) causes the progressive loss of central vision and is the most common cause of blindness in the elderly in industrialized nations (Tielsch *et al.*, 1995; Attebo *et al.*, 1996). Phenotypically, AMD is characterized by yellow extracellular deposits of proteins and lipids (drusen) that accumulate between the basolateral side of the retinal pigmented epithelium (RPE) and Bruch's membrane (de Jong, 2006). AMD etiology is complex and is influenced by age-related and environmental changes in the eye, including diminished antioxidant capacity, increased protein misfolding/aggregation, RPE apoptosis, and complement activation (Stone *et al.*, 2001).

Owing to the numerous factors influencing AMD progression, we hypothesized that studying an early-onset, inherited macular dystrophy, malattia leventinese/Doyne honeycomb retinal dystrophy (ML/DHRD), which phenotypically resembles AMD, may provide insight into the underlying causes of AMD (Piguet *et al.*, 1995; Marmorstein, 2004; Kundzewicz *et al.*, 2008). ML/DHRD is caused by a single Arg345Trp (R345W) mutation in the sixth epidermal growth factor (EGF) domain of the EGF-containing, fibulin-like extracellular matrix protein 1 (EFEMP1; Figure 1A; Stone *et al.*, 1999). Patients with ML/DHRD present with clinical and pathological AMD-like symptoms, including soft drusen accumulation, the loss of basolateral ruffling of the RPE, RPE vacuolization, and atrophy, as

This article was published online ahead of print in MBoC in Press (http://www.molbiolcell.org/cgi/doi/10.1091/mbc.E11-08-0695) on October 26, 2011.

Address correspondence to: John D. Hulleman (hulleman@scripps.edu) or Jeffery W. Kelly (jkelly@scripps.edu).

Abbreviations used: AMD, age-related macular degeneration; BNPS-skatole, 2-(2-nitrophenylsulfenyl)-3-methyl-3′-bromoindolenine; CHX, cycloheximide; DPBS, Dulbecco's phosphate-buffered saline; EFEMP1, epidermal growth factor–containing, fibulin-like extracellular matrix protein 1; EGF, epidermal growth factor; ER, endoplasmic reticulum; GLuc, *Gaussia* luciferase; HEK-293T, human embryonic kidney cells; ML/DHRD, malattia leventinese/Doyne honeycomb retinal dystrophy; RPE, retinal pigmented epithelium.

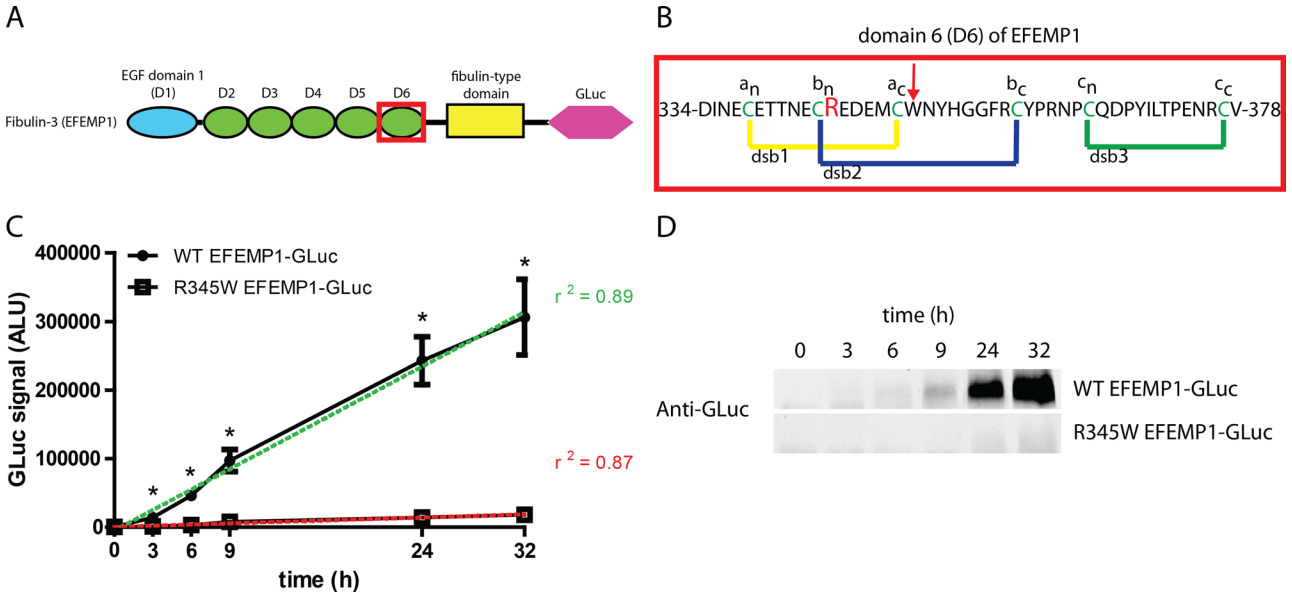

FIGURE 1: *Gaussia* luciferase (GLuc) fusion to EFEMP1 serves as a sensitive and robust reporter. (A) Schematic of fibulin-3 (EFEMP1). EFEMP1 is composed of one Ca^{2+}-binding EGF domain with an extra insertion (blue oval), five Ca^{2+}-binding EGF domains (green ovals), and a fibulin-type domain (yellow rectangle). These domains are followed the addition of a C-terminal GLuc (pink hexagon). The R345W mutation is located in domain 6 (red box). (B) Domain 6 sequence of EFEMP1. Three predicted native disulfide bonds (dsb1, dsb2, and dsb3) are in yellow, blue, and green, respectively. Each cysteine is colored green and is assigned a designation (a, dsb1; b, dsb2; etc.) and its location relative to the N or C terminus (a_n is the cysteine involved in dsb1, and, of the two cysteines involved in dsb1, is closer to the N-terminus). Arg-345, which is mutated to Trp in ML/DHRD, is colored red. The location of BNPS-skatole cleavage within non-R345W mutants is shown with a red arrow. (C) R345W EFEMP1-GLuc is secreted less efficiently than WT EFEMP1-GLuc. HEK-293T cells were transfected for 16 h, after which the media was replaced. The extracellular accumulation of the GLuc fusion protein was monitored for up to 48 h after transfection (n = 3, ±SD, *$p < 0.05$, WT EFEMP1-GLuc vs. R345W EFEMP1-GLuc, *t* test). (D) Western blot analysis of secreted EFEMP1-GLuc. A total of 50 µl of conditioned media (containing 2% FBS to prevent distortion from bovine serum albumin) was subjected to Western blotting and probed with an anti-GLuc antibody. Representative data of three independent experiments are shown.

well as eventual neovascularization on an accelerated time frame, usually during the fourth decade of life (Young, 1987; Piguet *et al.*, 1995; Stone *et al.*, 1999; de Jong, 2006; Jager *et al.*, 2008). Mutations in other homologous fibulin genes (fibulin-5 and -6) have been associated with an increased chance of developing AMD (Schultz *et al.*, 2003; Mullins *et al.*, 2007).

EFEMP1 is a monomeric, seven-domain, disulfide-rich, secreted extracellular matrix (ECM) glycoprotein (Figure 1A; Zhang and Marmorstein, 2009) that is expressed throughout the body, including in the brain, lung, placenta, heart, and RPE (Timpl *et al.*, 2003). EFEMP1 contains canonical tandem arrays of calcium (Ca^{2+})-binding EGF domains (D1–D6) followed by a C-terminal fibulin-type domain (Figure 1A; Zhang and Marmorstein, 2009). The functions of the fibulin family of proteins, including EFEMP1, are largely unknown. Mouse knock-out studies indicate that the fibulins are crucial for cellular integrity by regulating elastogenesis and vascularization and may serve as a link between cell surface receptors and ECM elastic fibers (Kostka *et al.*, 2001; Timpl *et al.*, 2003; McLaughlin *et al.*, 2006, 2007).

Mice lacking EFEMP1 do not develop any observable ML/DHRD or AMD-like phenotype (McLaughlin *et al.*, 2007). However, removal of EFEMP1 hastened the aging process and significantly disrupted elastic fibers. Consistent with a gain-of-toxic-function origin for ML/DHRD, R345W EFEMP1 knock-in mice develop sub-RPE membranous drusen-like deposits that increase with age and mutant EFEMP1 copy number, eventually resulting in RPE degeneration, vacuolization, and complement activation (Fu *et al.*, 2007; Marmorstein *et al.*, 2007). Studies indicate that the R345W mutation leads to an apparent EFEMP1 secretion deficiency and intracellular accumulation of mutant EFEMP1 (presumably in the endoplasmic reticulum [ER]; Marmorstein *et al.*, 2002). Subsequent cellular studies noted that R345W EFEMP1 expression caused an increase in the levels of vascular endothelial growth factor, the ER chaperone, glucose-regulated protein 78 (BiP), and spliced X-box binding protein 1, together indicating activation of the unfolded protein response (UPR) (Roybal *et al.*, 2005; Ron and Walter, 2007).

However, no studies have addressed the molecular basis underpinning how the R345W EFEMP1 mutation causes ML/DHRD. It is not known whether the dysfunction caused by the mutant is due to its intracellular misfolding and higher intracellular steady-state levels or whether the etiology is a consequence of the small amount of extracellular accumulation of misfolded and/or aggregated mutant EFEMP1, or both. Thus it is unclear whether enhancing mutant EFEMP1 folding and secretion to the ECM or if reducing mutant EFEMP1 secretion by degrading it by enhanced ER-associated degradation and/or autophagy within the cell would be a better strategy to slow the progression of or reverse ML/DHRD (Werner *et al.*, 1996; McCracken *et al.*, 1998).

The concept of proteostasis maintenance is central to understanding the cause of macular dystrophy and for developing strategies by which it can be remedied (Balch *et al.*, 2008; Evans *et al.*, 2010; Sifers, 2010). Proteostasis refers to proper proteome maintenance orchestrated by a cell to ensure successful development and aging. Proteostasis is constantly monitored by stress-responsive

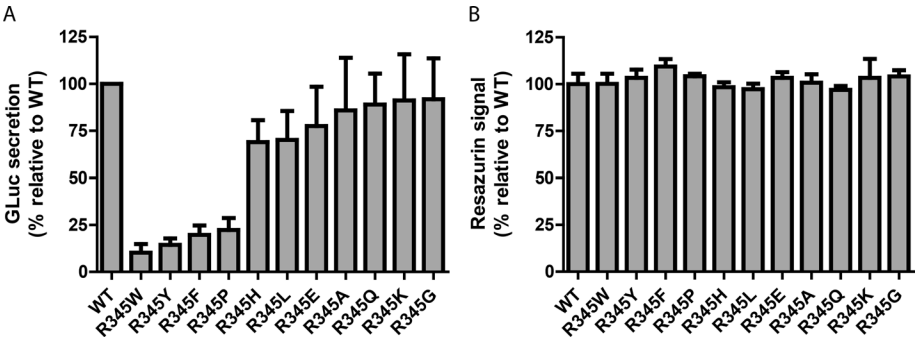

FIGURE 2: GLuc luminescence assay of secreted WT EFEMP1-GLuc and R345 EFEMP1-GLuc mutants transfected into HEK-293T cells. (A) Aromatic amino acid substitutions at R345 cause secretion defects. Aliquots of 45 µl of conditioned media from transfected HEK-293T cells were taken 72 h after transfection (24 h after a media change) and assayed for the presence of the EFEMP1-GLuc fusion protein. ($n \geq 3$, ±SD). (B) Inefficiently secreted EFEMP1-GLuc variants do not cause toxicity in HEK-293T after 72 h of expression. Transfected cells were assessed for differences in metabolic activity using the redox-sensitive dye, resazurin ($n = 4$, ±SD).

signaling pathways in distinct subcellular compartments to match the proteostasis capacity to demand by using transcriptional programs and translational control. Transcriptional up-regulation of proteostasis components enhances chaperone- and enzyme-mediated folding, vesicular trafficking, and degradation capacity mediated by the proteasome and/or the lysosome (Balch *et al.*, 2008; Evans *et al.*, 2010). As such, the maintenance of proteostasis prevents disease onset and influences cellular survival during development and aging. Conversely, a loss of cellular proteostasis is synonymous with aberrant protein folding, compromised protein trafficking and secretion, and/or the buildup of undegraded/mistrafficked or undegraded/aggregated proteins within the cell. Sustained proteostasis insufficiency, linked to UPR signaling, can lead to apoptosis (Tabas and Ron, 2011). We hypothesized that cells expressing mutant EFEMP1 exhibit a reduction in their capacity to fold and properly secrete the mutant protein. We propose that the cellular environment governing R345W EFEMP1 proteostasis can be adapted to avert ML/DHRD, as demonstrated with other cellular models of protein misfolding diseases (Mu *et al.*, 2008; Wang *et al.*, 2008; Cohen *et al.*, 2009; Hutt *et al.*, 2010).

To sensitively monitor how mutant EFEMP1 folding and secretion respond to changes in the proteostasis network, we developed a cell-based assay in which we fused EFEMP1 to *Gaussia* luciferase (GLuc; Tannous *et al.*, 2005). EFEMP1-GLuc secretion in human embryonic kidney cells (HEK-293T cells) can be monitored in real time by quantification of its secretion into the media relative to its intracellular accumulation. By using a series of R345 mutants, we demonstrate that the cause of inefficient secretion is the introduction of a large aromatic residue at position 345 next to a native disulfide bond, which leads to deficiencies in the ability of domain 6 to form its requisite disulfide bonds for secretion (Figure 1B; Sevier and Kaiser, 2002). Moreover, we establish two methods to enhance proteostasis network capacity (temperature reduction and chemically mediated translational attenuation) that alleviate the secretion defects caused by R345W and other bulky side chain mutations, enhancing mutant secretion up to fourfold.

RESULTS

Fusion of EFEMP1 to GLuc serves as a convenient and sensitive luminescence method to monitor EFEMP1 secretion

As an alternative to pulse chase experiments used previously to quantify EFEMP1 secretion (Marmorstein *et al.*, 2002), we fused EFEMP1 to GLuc to report on its extracellular versus intracellular localization. To test whether the EFEMP1-GLuc fusion proteins were secreted similar to what was reported for wild-type (WT) and R345W EFEMP1, HEK-293T cells were transiently transfected with EFEMP1-GLuc–encoding constructs and the secretion of WT EFEMP1-GLuc and R345W EFEMP1-GLuc was followed over time by assaying for GLuc activity in the media. Three hours after a media change (19 h after transfection), WT and R345W EFEMP1-GLuc were detectable in the media (Figure 1C). At 3 h, ~13 ± 3.2–fold more WT EFEMP1-GLuc was observed relative to R345W EFEMP1-GLuc (Figure 1C). The WT and R345W EFEMP1-GLuc media concentrations continued to increase linearly over the time course of the experiment, with WT EFEMP1-GLuc levels peaking at ~16 ± 0.36–fold higher than those of R345W EFEMP1-GLuc 24 h after the media change (Figure 1C).

To assess the sensitivity of the GLuc assay, we performed Western blotting on conditioned media samples. Whereas the luciferase assay detected WT EFEMP1-GLuc as early as 3 h after the media change, Western blotting was only able to detect the fusion protein 9 h after the media change, corresponding to a luciferase assay readout of ~100,000 ALU, a signal ~200 times greater than our designated minimum detectible GLuc signal of 500 ALU (compare Figure 1D to 1C). Secreted R345W EFEMP1-GLuc accumulated to a much lower extent in the media than WT EFEMP1-GLuc by Western blot analysis (Figure 1D), consistent with quantification using the GLuc assay (Figure 1C). Of note, the levels of R345W EFEMP1-GLuc barely reached the limit of detection using Western blotting (Figure 1D).

To ensure that the folding and secretion differences we observed between WT and R345W EFEMP1-GLuc were not due simply to differences in transfection efficiency or transcript levels, we performed quantitative real-time PCR. No significant differences in transcript levels of EFEMP1 or GLuc were observed in HEK-293T cells transfected with either WT or R345W EFEMP1-GLuc (Supplemental Figure S1, A and B). In general, EFEMP1 transcript levels were found to be 100–300 times higher in cells transfected with EFEMP1-GLuc plasmids than in untransfected controls, indicating significant EFEMP1 overexpression (Supplemental Figure S1A).

Aromatic amino acid substitutions at position 345 result in inefficient EFEMP1 secretion

To gain insight into the molecular basis for the poor secretion of R345W EFEMP1, side chain hydrophobicity, size, charge, and side chain influence on backbone conformation were varied at the R345 position by mutagenesis. We generated 10 position 345 variants of EFEMP1-GLuc (in addition to R345W) and monitored the secretion efficiency of these variants relative to WT EFEMP1-GLuc 24 h after a media change (72 h after transfection; Figure 2A). Mutation from the native arginine residue, which is positively charged at physiological pH, to an uncharged residue bearing a relatively small side chain (R345A) or to an uncharged residue bearing no side chain and exhibiting maximal local backbone conformational flexibility (R345G) had no detrimental effect on secretion efficiency relative to WT EFEMP1-GLuc (86 ± 28% and 92 ± 22%, respectively; Figure 2A). Altering the Arg side chain to a similarly sized polar and conformationally flexible side chain, including uncharged glutamine (R345Q,

89 ± 17%; Figure 2A) or charged lysine (R345K, 91 ± 25%) did not reduce folding and secretion efficiency notably either. Mutation to a similarly sized, hydrophobic uncharged side chain (leucine, R345L, 70 ± 15%; Figure 2A) slightly reduced secretion compared with WT EFEMP1-GLuc. Surprisingly, reversal of the positive charge on the side chain of arginine to the negative charge on the side chain of glutamic acid (R345E) did not lower EFEMP1 secretion substantially either (78 ± 21%; Figure 2A). In contrast, mutating R345 to a large aromatic side chain, including tyrosine (R345Y, 15 ± 3.4%; Figure 2A) and phenylalanine (R345F, 20 ± 5.0%) dramatically reduced secretion efficiency, analogous to what was observed with the R345W pathological EFEMP1 mutant (10 ± 4.7%; Figure 2A). Mutation of R345 to the smaller heteroaromatic imidazole side chain of histidine (R345H) also reduced EFEMP1 secretion (69 ± 12%; Figure 2A), albeit to a lesser extent than the larger aromatic side chains. Mutation of R345 to an uncharged cyclic proline residue (R345P) was almost as devastating to EFEMP1 secretion as mutation to phenylalanine (22.4 ± 6.3%; Figure 2A), probably due to the restricted backbone conformation of proline ($\phi = -65°$; Williamson, 1994).

To eliminate a possible alternative explanation for the secretion differences observed among the variants of EFEMP1-GLuc studied, we assessed the cell toxicity caused by these mutants, as cytotoxicity would lead to an apparent decrease of secretion of EFEMP1 into the media. Cellular viability was assessed 72 h after transfection by employing the 7-hydroxy-3H-phenoxazin-3-one 10-oxide (resazurin) assay, which reports on mitochondrial redox potential. On the basis of this often-used assay for cytotoxicity (Usui *et al.*, 2009), none of the R345 EFEMP1-GLuc mutants generated were toxic to HEK-293T cells (Figure 2B).

We also controlled for the possibility that transfection efficiency differences could explain lower apparent secreted EFEMP1 mutant levels. To explore this possibility, another secreted luciferase (*Cypridina* luciferase [CLuc]) was cotransfected with the EFEMP1-GLuc constructs (Supplemental Figure S2). The secretion trends described earlier without CLuc normalization (Figure 2A) persisted with CLuc normalization (Supplemental Figure S2), demonstrating that none of the trivial explanations for the secretion differences observed appear to be valid. The CLuc cosecretion data also demonstrate that mutant EFEMP1-GLuc does not nonspecifically reduce secretion capacity from the ER under these transient transfection conditions.

Mutations leading to inefficient secretion of EFEMP1 are underrepresented at the b_n + 1 position of other Ca^{2+}-binding EGF domains in the fibulin family

The pathogenic EFEMP1 mutation position is located immediately adjacent to cysteine residue 344 (C344), which is required to form disulfide bond 2 of domain 6 (dsb2; Figure 1B). Disulfide bond 2 is predicted to be critical for the folding and function of the Ca^{2+}-binding EGF domain (Chang *et al.*, 1995, 2001). We hypothesized that compromised disulfide bond formation could play a part in reducing R345W EFEMP1 secretion efficiency. Comparative analysis of the amino acid residues present at the b_n + 1 location in 40 nonmutated Ca^{2+}-binding EGF domains from six different fibulin proteins indicates that none contain tryptophan, tyrosine, or phenylalanine and only one contains proline (Supplemental Tables SI and SII). Thus, of the four residues at position 345 that cause defects in EFEMP1 secretion (Trp, Phe, Tyr, and Pro), only proline is found in one of the 40 domains analyzed (domain 4 in fibulin-1, Supplemental Tables SI and SII). If the amino acid type at position 345 were determined statistically, then these four residues (Trp, Phe, Tyr, Pro) would be expected to occupy eight of the 40 possible domains, yielding an occupancy rate of 20%, a number far greater than the observed occupancy of 2.5% at this position (Supplemental Table SII). Mutations at the b_n + 1 position that modestly affect secretion (R345H, R345L, and R345E) are present in five domains (12.5%), close to the predicted 15% occupancy. Of the 34 remaining domains, 25 are preferentially occupied at the b_n + 1 position by glutamine (nine domains), arginine (seven domains), or serine (seven domains), accounting for 62.5% of the residues at this position. Our data indicate that at least two of these three prominent amino acids are well tolerated at position 345 and have relatively similar secretion efficiencies (Figure 2A; serine not evaluated). Although the sequence analysis of the evolutionary record and experimental sequence-dependent secretion data correlate well, an exception is lysine, which is not found in the b_n + 1 position in any of the 40 domains studied (Supplemental Table SI and SII), yet its secretion efficiency is indistinguishable from that of WT (Figure 2A).

Inefficient secretion by EFEMP1 mutants is improved by lowered cell growth temperatures

The misfolding/aggregation and/or increased steady-state retention of several disease-associated proteins at 37°C within cells can be rescued by reducing the cellular growth temperature from 37 to 27–33°C (Kulka *et al.*, 1988; Michalovitz *et al.*, 1990; Denning *et al.*, 1992; Wang *et al.*, 2008). To determine whether the poor secretion of the R345W mutation could be improved by a shift to lower temperatures, we reduced the growth temperature of WT- or mutant-expressing HEK-293T cells to 30°C for up to 24 h. Within 3 h of the temperature shift, significantly more R345W (relative to WT) was secreted to the media, increasing from 11 to 24% of WT levels (Figure 3A). Secretion was enhanced over the span of 24 h, peaking at ~53% of WT secretion at 24 h, whereas R345W secretion at 37°C remained at ~10% of WT levels under identical conditions (Figure 3A).

We also examined whether the cellular secretion of the additional R345 point mutants was temperature sensitive. A lower (permissive) temperature of 30°C significantly enhanced the secretion of the R345Y, R345F, R345P, R345L, and R345E variants, raising the relative secretion percentage from a range of 10–82% at 37°C to 47–104% at 30°C 24 h after temperature shift (Figure 3B). Of interest, R345W was still secreted most poorly, followed by R345Y and R345F (Figure 3B). A comparison of the total amount of EFEMP1 secreted at 24 h based on measured luminescence values (not relative to WT) is presented in Supplemental Figure S3, revealing a strictly analogous picture.

Identically treated samples were subjected to Western blot analysis (Figure 3C) to verify the validity of the GLuc assay results (Figure 3B). At 37°C, the inefficiently secreted and presumably misfolded EFEMP1 mutants, R345W, R345Y, R345F, and R345P were barely detectable (Figure 3C). In agreement with the GLuc assay, levels of these fusion proteins in conditioned media were significantly enhanced by growth at the permissive temperature (Figure 3C). Quantification of the integrated band intensities was performed, revealing that the GLuc luminescence and Western blot band intensities were in agreement (Supplemental Figure S4A). Furthermore, GLuc luminescence correlated linearly with EFEMP1 protein concentration, as determined by LI-COR quantification (Supplemental Figure S4B).

Inefficiently secreted variants accumulate intracellularly

To account for the remainder of the R345 aromatic- and R345 proline-containing EFEMP1-GLuc mutants that was not secreted, we also assessed their intracellular abundance. The four mutants that exhibited the largest secretion deficiencies accumulated intracellularly up to two times the levels of WT under identical steady-state conditions at 37°C, whereas intracellular levels of the remaining mutants hovered

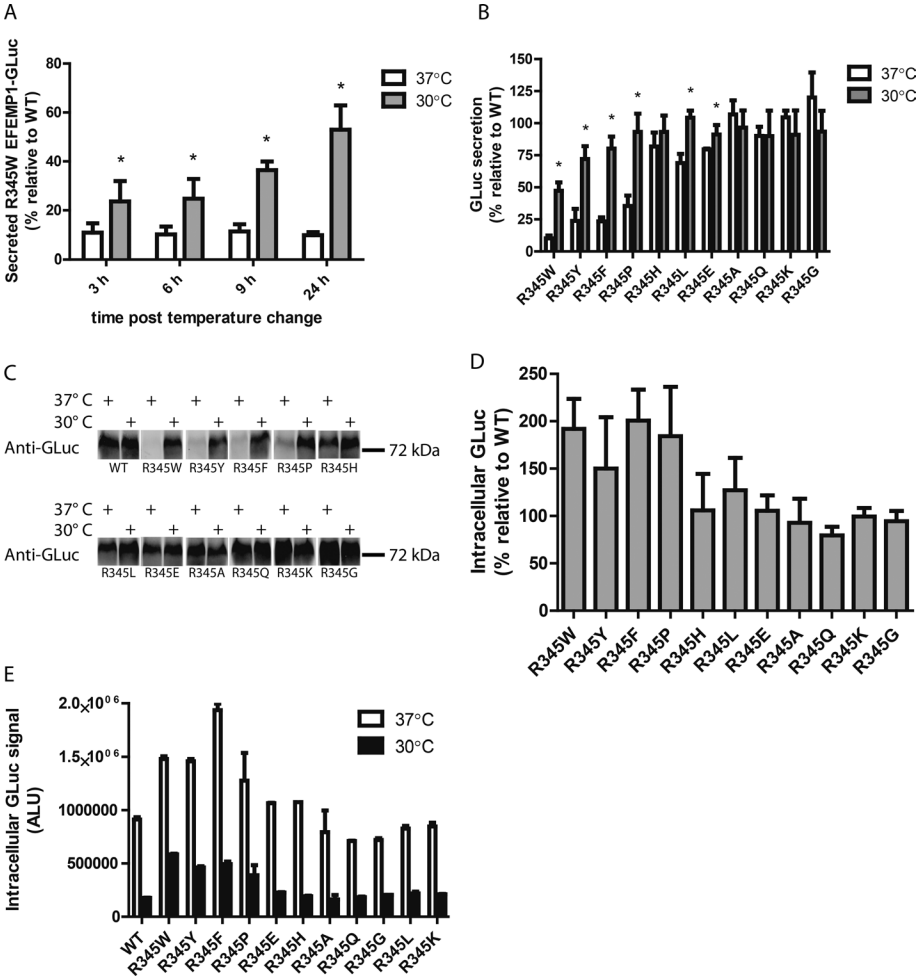

FIGURE 3: Secretion of EFEMP1 mutants is temperature sensitive. (A) HEK-293T cells were transfected for 48 h at 37°C, followed by a media change and temperature shift to 30°C for up to 24 h. Aliquots were taken at the indicated intervals after the temperature shift (denoted as t = 0 h) and assayed by the GLuc assay (n ≥ 3, ±SD). (B) Secretion defects caused by aromatic residues at R345 are partially rescued by growth at permissive temperatures. HEK-293T cells were transfected as described in A and were transitioned to 30°C for 24 h. After the temperature shift, aliquots of conditioned media were used in the GLuc assay (n = 4, ±SD, *p < 0.05, 37°C vs. 30°C, *t* test). (C) GLuc assay results are paralleled by Western blotting. Samples from the GLuc assay in B were analyzed by reducing SDS–PAGE, followed by Western blotting for the GLuc antigen as described in Figure 1D. Representative data of two independent experiments are shown. (D) The extent of intracellular accumulation of EFEMP1-GLuc variants is inversely proportional to secretion efficiency. Cells were transfected with the indicated constructs for 48 h, followed by temperature shift and media change for 24 h prior to assaying for intracellular GLuc (n ≥ 3, ±SD). (E) Intracellular retention of inefficiently secreted mutants, while substantially lower, persists at reduced temperatures. Intracellular GLuc was assayed in transfected cells incubated at 37 or 30°C for 24 h. Representative data (mean ± SD of technical replicates) of at least three independent experiments are shown.

around WT levels (Figure 3D). Thus, consistent with observations made by other groups using complementary approaches (Marmorstein *et al.*, 2002), it appears that the poorly secreted mutants misfold/aggregate and thus exhibit higher steady-state intracellular levels while awaiting degradation, most likely by ER-associated degradation (Werner *et al.*, 1996; McCracken *et al.*, 1998). Of interest, the same intracellular steady-state accumulation trends are observed in cells grown at 30°C; however, the absolute levels of intracellular EFEMP1-GLuc are much lower, most likely due to enhanced secretion (removal of the intracellular protein pool) in combination with translational attenuation (Figure 3E). Intracellular mutant EFEMP1-GLuc retention relative to WT EFEMP1-GLuc at 30°C is depicted in Supplemental Figure S5, demonstrating a similarity in trends when compared with Figure 3E.

Translational attenuation slightly increases mutant EFEMP1-GLuc secretion

One proteostasis network adaptation that can occur at lower cellular growth temperatures is translational attenuation (Fujita, 1999). To address whether translational attenuation might contribute to the enhanced secretion of EFEMP1 mutants, transfected cells were treated with cycloheximide (CHX), which nonspecifically prevents translational elongation (Siegel and Sisler, 1963). Addition of a low concentration of CHX (1 μM) for 24 h did not result in significant cell death, acting as a means to more gently prevent protein translation when compared with typical CHX treatments (up to 50 μM for a few hours). CHX did not significantly affect the secretion of WT EFEMP1-GLuc at 37°C (Figure 4A). However, intracellular levels of WT decreased after CHX treatment, indicating a reduction in protein translation and a removal of protein from the intracellular pool (Figure 4B). These results suggest that the majority of secreted EFEMP1-GLuc over the period of the 24-h time course originates from the intracellular pool of EFEMP1 already synthesized (not newly synthesized). Of interest, treatment of cells expressing WT EFEMP1-GLuc with CHX in combination with temperature reduction caused a significant reduction in secreted WT protein (to 65% of untreated WT levels; Figure 4A). Addition of CHX to cells expressing R345W EFEMP1-GLuc cultured at 37°C significantly enhanced R345W secretion by greater than twofold over untreated R345W-expressing cells at the same temperature (13 ± 1.7% without CHX vs. 28 ± 11% with CHX; Figure 4A). However, the extent of CHX-mediated rescue at 37°C was much lower than permissive temperature-mediated rescue (Figure 4A). Combining CHX and permissive temperature did not provide a synergistic or additive effect (Figure 4A), likely because temperature reduction already results in translational attenuation.

To determine whether translational attenuation generally enhanced the secretion of poorly secreted mutants, we analyzed the effect of CHX on the secretion of the other R345 variants at 37°C. CHX treatment also significantly enhanced the secretion of other presumably misfolded/aggregated mutants, including R345Y, R345F, R345P, and R345L, yet had no effect on R345 mutants that normally secrete efficiently (R345A, R345Q, R345K, R345G; Figure 4C).

Native disulfide bonds are required for proper EFEMP1 secretion

The formation of three disulfide bonds (Figure 1B) is generally critical for the proper folding of EGF domains and other small,

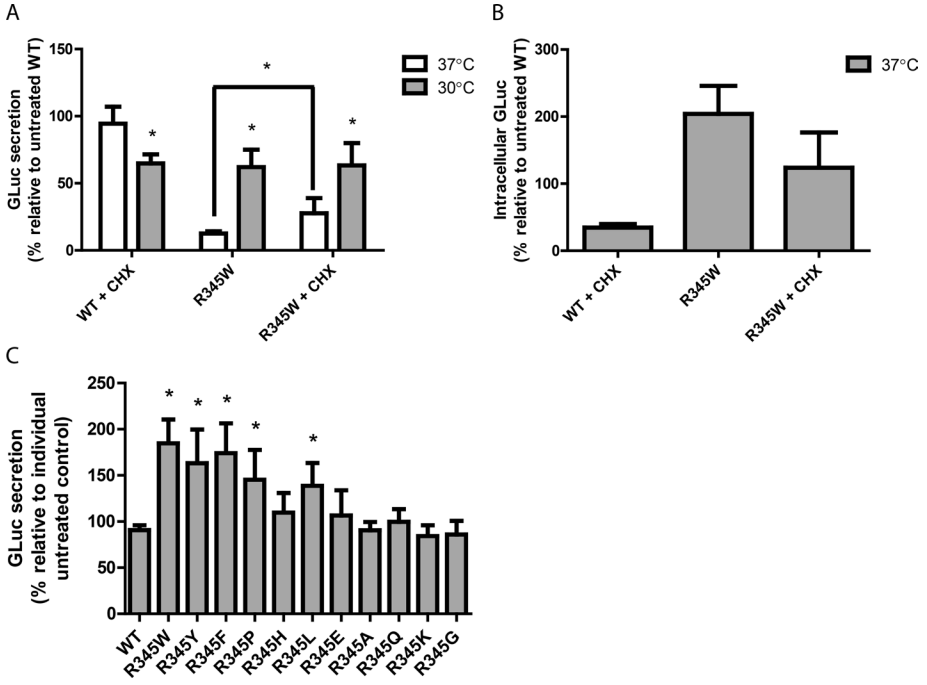

FIGURE 4: Translational attenuation with CHX subtly increases mutant EFEMP1 secretion. (A) HEK-293T cells were transfected with either WT or R345W EFEMP1-GLuc for 48 h at 37°C, followed by a media change and addition of 1 μM CHX and/or temperature shift to 30°C for up to 24 h. Aliquots of 45 μl of conditioned media were taken 24 h after the temperature shift/CHX treatment and assayed for EFEMP1-GLuc by the GLuc assay (n = 3, ±SD, *$p < 0.05$, 37 vs. 30°C, and +CHX vs. –CHX, *t* test). (B) CHX reduces intracellular EFEMP1 levels. HEK-293T cells were transfected with the indicated constructs for 48 h, followed by assaying for intracellular GLuc accumulation using the GLuc assay (n ≥ 3, ±SD). (C) Secretion defects in mutants other than R345W EFEMP1-GLuc are rescued by translational attenuation also. Transfected cells were treated with 1 μM CHX for up to 24 h at 37°C. Aliquots of 45 μl of conditioned media were taken for the GLuc assay (n = 4, ±SD, *$p < 0.05$, WT EFEMP1-GLuc vs. R345 mutants, *t* test).

disulfide-rich proteins (Chang *et al.*, 1995, 2001; Bulaj and Goldenberg, 1999). Specifically, we evaluated whether three native disulfide bonds were necessary for the folding and secretion of EFEMP1 (Sevier and Kaiser, 2002). We systematically eliminated each disulfide bond in domain 6 using individual Cys-to-Ala mutants (C338A, C359A, and C377A) in the WT and R345W EFEMP1-GLuc backgrounds. All cysteine mutants in both sequence backgrounds showed a significant defect in secretion efficiency when compared with their respective controls (Figure 5A). In addition, intracellular steady-state levels of all cysteine variants were enhanced relative to WT, as expected (Figure 5B). To address the concern that the observed secretion deficiencies could be due to the generation of orphan cysteines that could form incorrect or nonnative disulfide bonds, we constructed a double-cysteine mutant (C344A/C359A) that is incapable of forming dsb2. This variant acted identically to the other, single-cysteine mutants (Figure 5, A–C), demonstrating the necessity of dsb2 for proper EFEMP1 secretion.

Temperature reduction exhibited no positive effect on the secretion efficiency of any of the Cys-to-Ala EFEMP1 mutants (Figure 5C). These results demonstrate that a permissive temperature most likely improves the folding, secretion, and disulfide-bond formation fidelity of difficult-to-fold EFEMP1 mutants, but, of importance, a permissive temperature does not simply allow misfolded EFEMP1 or EFEMP1 missing a disulfide bond to exit the ER. This information, along with nonreducing Western blot analysis of secreted WT and R345W EFEMP1-GLuc (Supplemental Figure S6), suggests that the R345W and other EFEMP1-GLuc mutants that are secreted into the media most likely contain their native disulfide bonds and demonstrates the importance of proper disulfide bonding in domain 6 for proper folding and secretion.

2-(2-Nitrophenylsulfenyl)-3-methyl-3′-bromoindolenine cleavage of EFEMP1 reflects the presence or absence of dsb2 in domain 6

Within the WT EFEMP1-GLuc fusion protein, there are three tryptophan residues (see Supplemental Figure S7 for schematic). One is located near the amino terminus of EFEMP1 (W35). The second Trp is positioned near the carboxy terminus of the GLuc domain (corresponding to W652). The third Trp is W351 (Figure 1B, red arrow), which is located in domain 6 between the cysteine residues that form dsb2, the disulfide bond that we hypothesize is disrupted in the R345W mutant. We therefore reasoned that cleavage of mutant EFEMP1-GLuc fusion proteins with 2-(2′-nitrophenylsulfenyl)-3-methyl-3-bromoinolenine (BNPS-skatole), a reagent that cleaves the C-terminal peptide bond following tryptophan residues, might provide insight into the formation of disulfide bonds or lack thereof in domain 6 of mutant versus WT EFEMP1.

BNPS-skatole cleavage at W35 is predicted to have only a minimal effect on the molecular weight of the EFEMP1-GLuc fusion protein (a 2.2-kDa loss; see Supplemental Figure S7 for a schematic of the expected cleavage products with and without an intact dsb2). Cleavage after W652 in the GLuc portion of the fusion protein will not affect the molecular weight under nonreducing conditions, regardless of whether dsb2 is intact or not (Supplemental Figure S7), because W652 is bracketed by two cysteines (C561 and C657) that are predicted to form a disulfide bond in folded GLuc (Ferre and Clote, 2005). Hence, the BNPS-skatole cleavage product of EFEMP1 with dsb2 intact is predicted to have a molecular weight of 70.1 kDa under nonreducing conditions (2.2 kDa smaller than the full-length 72.3 kDa; see Supplemental Figure S7). However, if dsb2 or an intermediate disulfide bracketing W351 is missing, the EFEMP1-GLuc fusion protein will dissociate into two halves upon BNPS-skatole cleavage, affording a C-terminal fragment with a molecular weight of 35.6 kDa (residues 352 onward) and an N-terminal fragment exhibiting a molecular weight of 34.5 kDa (containing residues 36–351 of EFEMP1). As predicted, substantially more of the C-terminal 35.6-kDa cleavage product formed in BNPS-skatole–treated R345W EFEMP1-GLuc lysates than in WT EFEMP1-GLuc HEK-293T lysates under identical conditions (Figure 6A). Production of the cleavage product was dependent on the presence of BNPS-skatole (Figure 6A) and on disulfide bond formation, since WT EFEMP1 can form more of the cleavage products when its disulfide bonds are reduced (Supplemental Figure S8).

To identify which disulfide bond disruptions afford fragments on a nonreducing SDS–PAGE gel after BNPS-skatole cleavage, we examined lysates from cells transfected with the Cys-to-Ala EFEMP1 mutations. In the WT background, there was no significant increase in the BNPS-skatole cleavage products of the C338A and C377A

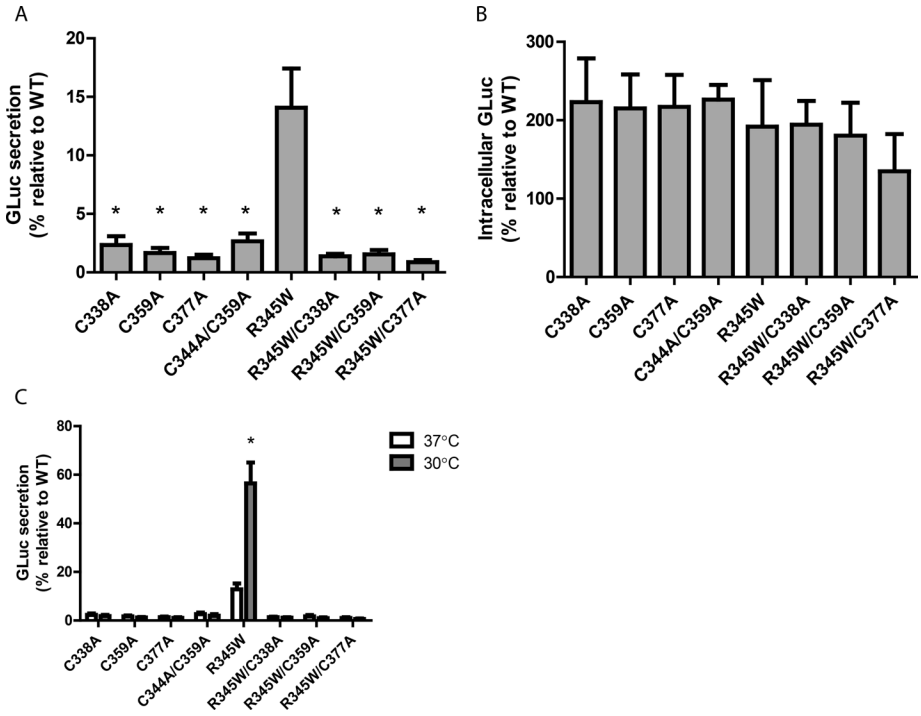

FIGURE 5: Cysteine residues are required for proper EFEMP1 secretion and temperature sensitivity. (A) EFEMP1 secretion is negated by cysteine residue mutation. Aliquots of 45 µl of conditioned media from transfected HEK-293T cells were taken 72 h after transfection and assayed for the presence of the EFEMP1-GLuc fusion protein (n = 3 ±SD, *p < 0.05, cysteine mutants vs. R345W EFEMP1-GLuc, *t* test). (B) Cysteine mutants accumulate intracellularly. HEK-293T cells were transfected with the indicated constructs for 72 h prior to assaying for intracellular GLuc accumulation (n = 3, ±SD). (C) Secretion of cysteine mutants is unaffected by temperature reduction. HEK-293T cells were transfected for 48 h, after which the media was changed and temperature reduced. Levels of EFEMP1-GLuc were quantified after 24 h at 37 or 30°C (n ≥ 3, ±SD, *p < 0.05, 37 vs. 30°C, *t* test).

variants when compared with WT (Figure 6, B and C), suggesting that the lack of dsb1 or dsb3 does not significantly influence the levels of cleavage product. In contrast, the C359A mutant, which eliminates a cysteine required for dsb2 formation, produced significantly more cleavage product than the other Cys-to-Ala mutants, indicating that BNPS-skatole cleavage reports largely on the absence of dsb2 (Figure 6, B and C), which is hypothesized to be incompletely formed in the R345W EFEMP1 mutant. It is intriguing that there is a portion of the C359A variant that is not cleaved after BNPS-skatole treatment. The remaining full-length C359A after BNPS-skatole cleavage is likely due to nonnative mixed disulfides, as increasing BNPS-skatole concentrations up to fourfold does not decrease full-length C359A band intensity (Supplemental Figure S9).

In the R345W background, the C338A mutation (eliminates dsb1) did not substantially alter the amount of BNPS-skatole cleavage product relative to R345W (Figure 6, B and C). In agreement with the C359A mutation in the WT background eliminating dsb2, the R345W/C359A variant also generated significantly more cleavage product than did R345W (Figure 6, B and C). These data suggest that some R345W EFEMP1-GLuc is capable of forming dsb2 (or bracketing intermediate disulfides), since without the C359A mutation substantially less R345W cleavage product is observed. Unexpectedly, the C377A mutation slightly lowered the amount of BNPS-skatole cleavage product relative to R345W (Figure 6, B and C), possibly indicating stabilization of one or more disulfide intermediates that bracket both W345 and W351. As expected, the levels of BNPS-skatole cleavage product of the cysteine mutants were effectively unaltered by temperature reduction (Supplemental Figure S10).

Poorly secreted EFEMP1 mutants exhibit alterations in disulfide bond formation within domain 6 of EFEMP1

In cell lysates, all R345 mutant EFEMP1-GLuc constructs treated with BNPS-skatole exhibited detectible amounts of cleavage product (Figure 7, A and B). The R345W mutation exhibited the most cleavage product (Figure 7, A and B) potentially due to the additional BNPS-skatole cleavage site, and/or less dsb2 formation, and/or fewer intermediate disulfide bonds surrounding the two tryptophans in domain 6 of R345W EFEMP1-GLuc (Figure 1B). Other poorly secreted mutants (R345Y, R345F, R345P) also exhibited a significantly higher level of the 35.6-kDa BNPS-skatole cleavage product when compared to R345G, a variant that secretes identically to WT (Figure 7, A and B), also hinting at a decrease in dsb2 formation and/or a decrease in disulfide intermediates bracketing W351 in other poorly secreted EFEMP1 mutants. Growth at permissive temperatures had no significant effect on the amount of BNPS-skatole cleavage product relative to full-length EFEMP1 in cell lysates for both WT and R345W EFEMP1-GLuc (Figure 7C), suggesting that once EFEMP1-GLuc has achieved proper disulfide formation, it is efficiently removed from the EFEMP1 intracellular pool and secreted into the media.

To determine more definitively whether secreted R345W had an enhanced ability to form dsb2 (or a disulfide bond surrounding W345 and W351), we treated conditioned media from cells grown at reduced temperature with BNPS-skatole and monitored the 35.6-kDa cleavage product (Supplemental Figure S11A). Although intracellular R345W EFEMP1-GLuc generated ~600% more BNPS-cleavage product than did WT (Figure 7, A and B), quantification of the fractional BNPS-skatole C-terminal cleavage product arising from secreted R345W EFEMP1-GLuc produced from cells grown at a permissive temperature suggests that R345W only has 86% more BNPS-skatole–sensitive cleavage product than WT (Supplemental Figure S11B), a substantial reduction in cleavage product when compared with intracellular R345W. These data, which may even overestimate the amount of cleavage in secreted R345W EFEMP1-GLuc relative to WT because of the miniscule amount of observed cleavage product (Supplemental Figure S11A), suggest that secreted R345W contains dsb2 or a disulfide that brackets W345 and W351, indicating that dsb2 formation is at least one factor that governs EFEMP1 secretion. These results are fully consistent with an enhanced ER folding environment at a permissive temperature for both WT and R345W EFEMP1 and thus more complete dsb2 formation in the ER, enabling enhanced proper folding and secretion.

DISCUSSION

Although mutations in fibulin genes homologous to EFEMP1 are linked to AMD, no mutations in EFEMP1 have been correlated

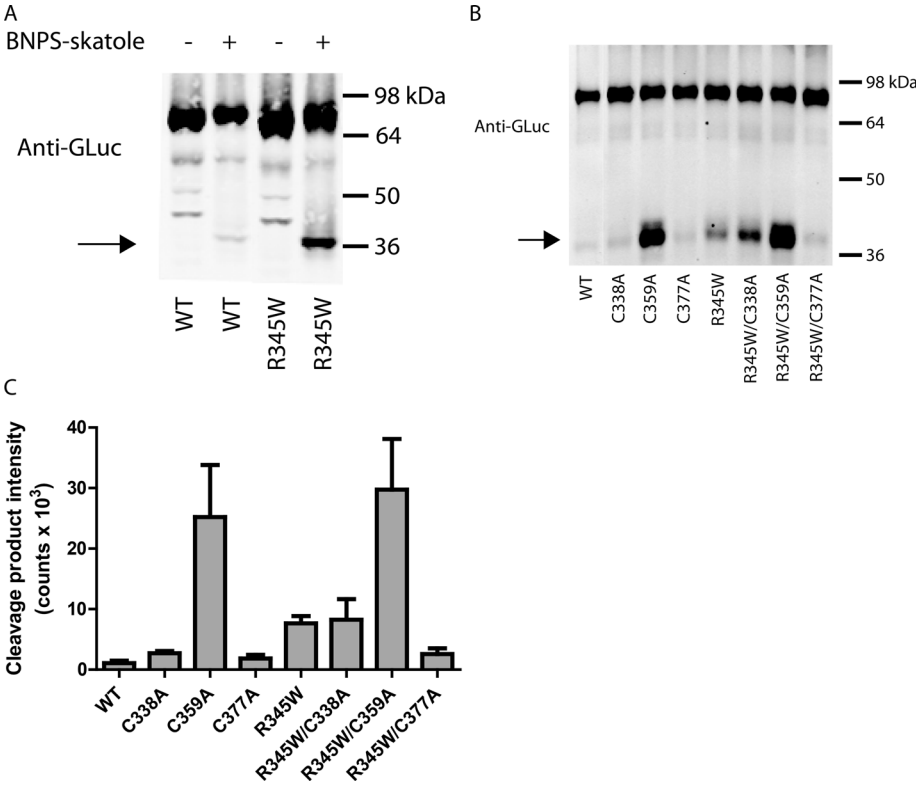

FIGURE 6: BNPS-skatole cleaves dsb2 in domain 6 of EFEMP1. (A) The domain 6 cleavage product is BNPS-skatole dependent. Lysates from transfected cells were treated overnight with either glacial acetic acid (−) or BNPS-skatole in glacial acetic acid (+) and were run on nonreducing SDS–PAGE, followed by Western blotting for the GLuc epitope. Representative data of three independent experiments are shown. (B) Lysates from transfected HEK-293T were treated overnight with BNPS-skatole and separated on a nonreducing SDS–PAGE gel followed by Western blotting as described in Figure 1D. BNPS-skatole cleavage product arising from the lack of a disulfide bond bracketing W351 is designated by an arrow. Representative data of three independent experiments are shown. (C) LI-COR quantification of the cleaved isoform presented in A. The intensity of the cleaved isoform (arrow) was quantified (n = 3, ±SD; C338A, n = 2, ±SD).

directly with development of AMD at this juncture. Yet it is clear from observations in humans (Bressler *et al.*, 1988; Piguet *et al.*, 1995) and knock-in mice (Fu *et al.*, 2007; Marmorstein *et al.*, 2007) that the R345W EFEMP1 mutation causes ML/DHRD, a disease that phenotypically resembles AMD on an accelerated time frame. In addition to the R345W disease-associated mutation, we demonstrate that two aromatic substitutions (R345Y and R345F) and one backbone conformationally restricted mutant (R345P) in EFEMP1 are folding and secretion compromised, analogous to R345W.

If the extent to which EFEMP1 secretion is reduced correlates with susceptibility of developing ML/DHRD, based on our data, mutations other than tryptophan could also cause disease. One explanation for why no other mutations have been reported at position 345 is that the natural arginine codon (CGG) would need to undergo a three–base pair change to be mutated to either tyrosine (TAT or TAC) or phenylalanine (TTT or TTC), an unlikely event. In contrast, only a one–base pair change is necessary for the tryptophan (TGG) or proline (CCG) mutations. At 37°C, R345P causes an approximate fourfold reduction in the secretion of EFEMP1 relative to WT. However, shifting the growth temperature to 30°C demonstrates that the R345P mutation is more easily tolerated than the aromatic substitutions, reaching 93% of secreted WT levels. Thus the cellular machinery responsible for folding EFEMP1 appears to be more responsive to a R345P substitution than to aromatic mutations, potentially averting a disease phenotype.

The time frame required for temperature reduction to enhance mutant EFEMP1 secretion (within 3 h) is consistent with the time scale required for a transcriptional enhancement of ER proteostasis capacity. Two genes known to be up-regulated by reduced temperature are protein disulfide isomerase (PDI) and ER protein 57 (ERp57; Baik *et al.*, 2006; Underhill and Smales, 2007), important proteostasis network components predicted to be beneficial in EFEMP1 secretion, given the compromised disulfide bond formation in the EFEMP1 mutants (Sevier and Kaiser, 2002). In fact, ERp57 has been shown to be involved in EFEMP1 folding (Jessop *et al.*, 2007). We speculate that up-regulation of these genes and/or their corresponding oxidoreductases, independent of temperature reduction, may be an alternative strategy for enhancing disulfide bonding fidelity linked to the folding and secretion of mutant EFEMP1 (Sevier and Kaiser, 2002; Sevier *et al.*, 2007).

A reduced cellular growth temperature, which is known to result in translational attenuation (Fujita, 1999), together with our CHX experiments, implies that translational attenuation enhances R345W EFEMP1 secretion. This is most likely realized through increasing the ratio of ER chaperones and folding enzymes to mutant EFEMP1, thereby promoting chaperone engagement and proper folding (Wang *et al.*, 2008). Because the CHX experiments were performed at 37°C, they provide hope that EFEMP1 secretion can be restored at physiological temperatures, in part by translational attenuation.

We hypothesize that hindered dsb2 formation results from the steric bulk of the neighboring aromatic side chain and/or from a neighboring residue that imposes a perturbation on the local backbone conformation. This hypothesis is supported by the lack of aromatic amino acids and the scarcity of proline residues occupying the $b_n + 1$ position in other Ca^{2+}-binding EGF domains. We do not suggest that placement of a tryptophan (or aromatic) residue immediately adjacent to a cysteine residue involved in disulfide bond formation is destabilizing or causes disulfide bond formation disruptions in a general fashion. Rather, it appears that the reduced dsb2 formation efficiency resulting from the presence of a bulky neighboring aromatic residue is EFEMP1 context dependent and most likely problematic because of the essential oxidative folding pathway of fibulin proteins.

In support of the EFEMP1 context–dependent aromatic disruption hypothesis, PDI, ERp57, and ER protein 72 (ERp72) all contain tryptophan residues immediately preceding the nucleophilic (N-terminal) cysteine in each of their critical Cys-Xaa-Xaa-Cys (CXXC) motifs required for catalysis of formation and isomerization of client protein disulfide bonds. Furthermore, aromatic residues (tryptophan and tyrosine, respectively) are also enriched immediately prior to CXXC/CXXS domains in thioredoxin homologues (Fomenko and Gladyshev, 2003) and methionine sulfoxide reductases (Fomenko

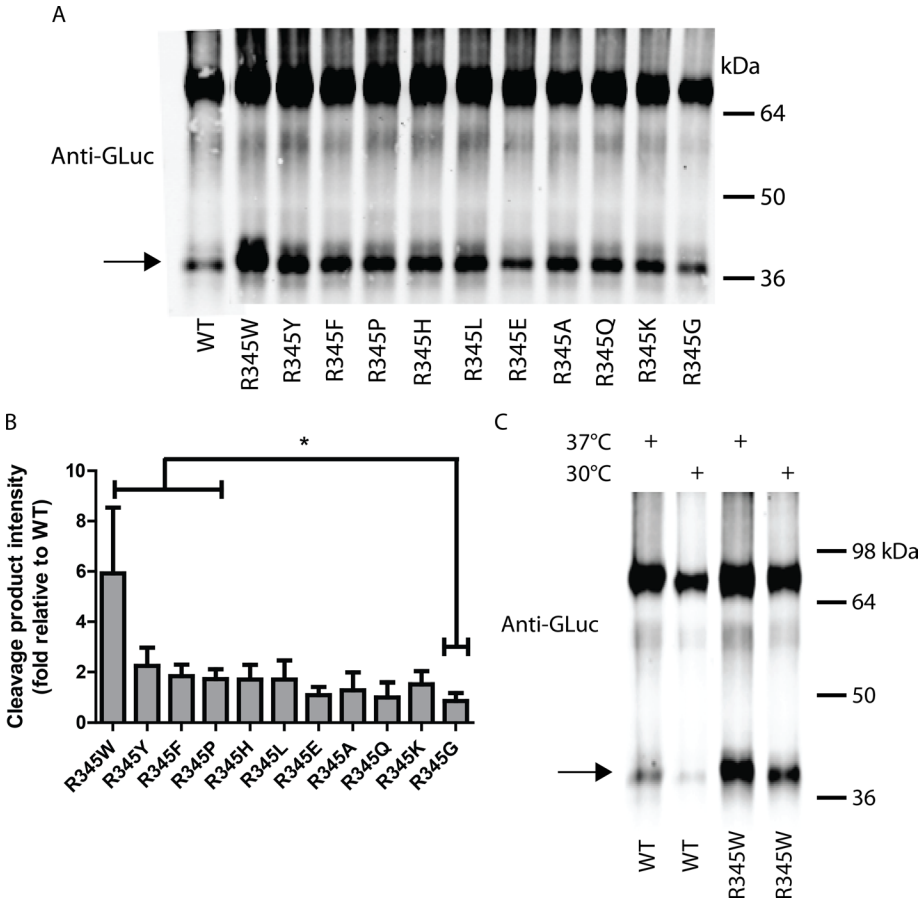

FIGURE 7: Poorly secreted R345 mutants lack proper disulfide bond formation in domain 6. (A) Lysates from transfected HEK-293T cells were treated overnight with BNPS-skatole and separated on a nonreducing SDS–PAGE gel, followed by Western blotting as described in Figure 1D. BNPS-skatole cleavage is designated by an arrow. Representative data of three independent experiments are shown. (B) LI-COR quantification of the cleaved isoform presented in A. The intensity of the cleaved isoform (arrow) was quantified (n = 3, ±SD, *$p < 0.05$, R345W, R345Y, R345F, and R345P vs. R345G, *t* test). (C) Reduced growth temperatures lower overall intracellular EFEMP1 levels but not the fractional percentage of cleaved product vs. full-length EFEMP1. Lysates from transfected HEK-293T cells were treated with BNPS-skatole after incubation at 37 or 30°C for 24 h. Representative data of three independent experiments are shown.

and Gladyshev, 2002), demonstrating the importance of aromatic residues in other structural contexts, potentially through S/π stabilization (Ringer *et al.*, 2007). These observations suggest that placement of aromatic residues near cysteines is likely critical for cysteine reactivity, possibly by pKa perturbation. Thus, in addition to sterically encumbering neighboring disulfide bond formation (dsb2) in the fibulin family of proteins, misplacement of tryptophan (such as the R345W mutation) or aromatic residues could also alter the reactivity of the flanking cysteine residue in the fibulins, creating abnormal disulfide-bonded intermediates. Clearly, further analysis of the disulfide bonding patterns of WT and R345W is warranted to understand the dynamics of disulfide bond formation in finer detail.

Although it seems clear that dsb2 formation is compromised, this may reflect a problem with R345W oxidative folding that runs deeper than the formation of one disulfide bond. The abundance of the BNPS-skatole–cleaved isoform does not account for all of the inefficiently secreted EFEMP1 protein but does appear to be an indication of folding problems within domain 6. It is important to note that the amount of BNPS-skatole cleavage product was not inversely proportional to secretion efficiency (i.e., poorly secreted mutants R345Y, R345F, and R345P did not have appreciably more cleaved product than the intermediately secreted mutants, R345H and R345L). Thus additional factors other than disulfide formation, such as the population of kinetic traps or differential interactions with ER-resident proteins/chaperones, may also affect the secretion of R345W EFEMP1.

In summary, the fusion of EFEMP1 to GLuc allows for the very sensitive and practical quantification of secreted (in the media) versus retained intracellular (in cell lysates) EFEMP1. Aromatic amino acids, including Trp, leading to macular dystrophy, compromise secretion, at least in part, by interfering with dsb2 formation and possibly the formation of other disulfide bond intermediates. It is clear from this work that R345W EFEMP1 is capable of fractional formation of dsb2 in cells grown at 37°C. Experiments performed at permissive growth temperatures and using chemically induced translational attenuation suggest that the adaptation of the proteostasis network at 37°C is likely to be effective at increasing R345W EFEMP1 folding and secretion while decreasing its intracellular accumulation and/or degradation. Future incorporation of mutant and WT EFEMP1-GLuc fusions in stable cell lines will allow us to determine more efficiently whether enhanced degradation of R345W EFEMP1 or its more efficient folding and secretion is a better strategy for ameliorating the macular dystrophy ML/DHRD.

MATERIALS AND METHODS

Construct generation

Full-length, untagged EFEMP1 variants were amplified by PCR from cDNA and were inserted into the pENTR1A Dual Selection vector (Life Technologies, Carlsbad, CA) using the *Eco*RI and *Xho*I restriction sites. A carboxy-terminal fusion with humanized GLuc (Tannous *et al.*, 2005) was generated by PCR amplification of EFEMP1 using primers that eliminated the natural stop codon of EFEMP1 and inserted a flexible, 16-residue linker (sequence, FEGSAGSAAGSGEFEA; Waldo *et al.*, 1999). This gene was then ligated to humanized GLuc (without a start codon or signal sequence). Fusion genes were inserted into the pENTR1A using the *Bam*HI (by way of *Bgl*II) and *Xho*I restriction sites. To generate EFEMP1 mutants, site-directed mutagenesis was performed using the QuikChange method (Agilent, Santa Clara, CA). Genes of interest were shuttled into the pcDNA-DEST40 vector by LR Clonase II recombination. All constructs were sequenced to verify their identity.

Cell culture

HEK-293T cells (Life Technologies) were cultured in high-glucose DMEM (Cellgro, Manassas, VA) supplemented with 10% (unless otherwise noted) heat-inactivated fetal bovine serum (FBS; Omega Scientific, Tarzana, CA) and 1% penicillin/streptomycin/glutamine (Cellgro). Cells were incubated at 37°C at 5% CO_2 (unless otherwise noted).

Introduction of EFEMP1 variants into HEK-293T cells was performed by transient transfection using FuGENE 6 or X-TremeGENE 9 (Roche, Nutley, NJ). For most experiments, cells were plated at a density of 50,000 cells/well in a 24-well plate and allowed to attach overnight. Cells were then transfected with the equivalent of 250 ng/well DNA (Qiagen, Germantown, MD) using 1.5 µl/well of transfection reagent for 24 h prior to replating/analysis. For cotransfections, each well was transfected with 250 ng of EFEMP1 DNA and 100 ng of control plasmid (encoding for *Cypridina* luciferase; New England Biolabs, Ipswich, MA).

For experiments in which reduced temperatures were used, HEK-293T cells were transfected for 24 h, replated at select densities, and allowed to attach at 37°C. Cell media was replaced 24 h after replating, followed by incubation at either 37 or 30°C for up to 24 h.

GLuc assay to monitor EFEMP1 secretion/intracellular accumulation

The secretion of EFEMP1-GLuc was monitored by adding 50 nl of substrate diluted in 10 µl of neat GLuc buffer (BioLux *Gaussia* Luciferase Assay Kit; New England Biolabs) to 45-µl aliquots of conditioned media (typically ~1/10 of the total media). Immediately after mixing, luminescence was measured in a 96-well Costar flat-bottomed black assay plate (Corning, Corning, NY) in a Safire II microplate reader (Tecan, Uppsala, Sweden) using a 100-ms integration time. For cotransfections, separate aliquots of conditioned media were taken and reacted with components of the BioLux *Cypridina* Luciferase kit (New England Biolabs) in an identical manner to the GLuc assay kit.

Intracellular accumulation of EFEMP1-GLuc was achieved by harvesting of cells (via trypsinization), pelleting of cells at ~10,000 × *g*, and resuspension in 100 µl of Dulbecco's phosphate-buffered saline (DPBS), followed by at least four times freeze/thaw in a dry ice/ethanol bath. Cell debris was pelleted by centrifugation at ~20,000 × *g* for 1 min. An aliquot (25–40 µl) was removed and used for the GLuc assay employing the same substrate/buffer ratio as described previously.

Western blotting

Equal volumes (50 µl) of conditioned media aliquots were denatured in reducing Laemmli buffer (unless otherwise indicated) by boiling at 95°C for 5 min, followed by loading onto a 10 or 12% SDS–PAGE gel. Proteins were transferred onto nitrocellulose membranes and blocked in 5% milk. The primary antibody used was a rabbit anti-GLuc (1:2000; New England Biolabs). Blots were imaged on a LI-COR Odyssey infrared imager (LI-COR, Lincoln, NE) using a goat anti-rabbit 800-nm secondary antibody (1:10,000; LI-COR).

Cell toxicity assay

HEK-293T cells were transfected with EFEMP1 constructs for 24 h, trypsinized, and then replated at ~4500 cells/well in a 96-well flat-bottom, clear Costar plate (Corning). Forty-eight hours after replating, cells were assessed for differences in metabolic activity by resazurin fluorescence changes. Briefly, 10 µl of resazurin (500 µM in PBS) was added to each well, and the plates were incubated for 2 h at 37°C. The fluorescence signal, which is proportional to cell metabolism/viability, was monitored on a Safire II microplate reader (Tecan; excitation wavelength, 530 nm; emission wavelength, 590 nm).

BNPS-Skatole cleavage of tryptophan residues in EFEMP1

BNPS-skatole cleavage was performed essentially as described previously (Crimmins *et al.*, 2005). HEK-293T cells were transfected with EFEMP1 constructs for 24 h, after which the media was changed and the cells were replated or allowed to grow for an additional 24–48 h. Cells were then treated with 20 mM iodoacetamide in DPBS for 30 min at 37°C. Cells were resuspended and lysed by freeze/thaw in dry ice/ethanol (at least four times). Cell debris and insoluble material was removed by centrifugation at ~20,000 × *g* for 5 min at 4°C. The remaining soluble portion (75 µl) was denatured with an equal volume of 8 M urea (dissolved in DPBS). Freshly prepared BNPS-skatole (250 µl, 1.6 mg/ml) in glacial acetic acid was added to the lysates. Samples were treated overnight at room temperature in the dark. Proteins were precipitated by adding 1.2 ml of cold acetone and incubating at −20°C for ≥2 h, followed by centrifugation at ~20,000 × *g* for 10 min at 4°C. Protein pellets were washed with acetone and respun at ~20,000 × *g* for 10 min at 4°C. Acetone was aspirated, and the pellet was air dried at room temperature for 30 min. Samples were then resuspended in 50 µl of 8 M urea in DPBS and heated to 95°C until the protein pellet redissolved. Proteins were further denatured in 1× nonreducing Laemmli buffer for 5 min at 95°C. Samples were then separated by SDS–PAGE, and Western blotting was performed as described.

ACKNOWLEDGMENTS

We thank R. Luke Wiseman for his insightful review of the manuscript. This work was supported by the Lita Annenberg Hazen Foundation, the Skaggs Institute for Chemical Biology, and Grant AG018917 from the National Institutes of Health awarded to J.W.K.

REFERENCES

Attebo K, Mitchell P, Smith W (1996). Visual acuity and the causes of visual loss in Australia. The Blue Mountains Eye Study. Ophthalmology 103, 357–364.

Baik JY, Lee MS, An SR, Yoon SK, Joo EJ, Kim YH, Park HW, Lee GM (2006). Initial transcriptome and proteome analyses of low culture temperature-induced expression in CHO cells producing erythropoietin. Biotechnol Bioeng 93, 361–371.

Balch WE, Morimoto RI, Dillin A, Kelly JW (2008). Adapting proteostasis for disease intervention. Science 319, 916–919.

Bressler NM, Bressler SB, Fine SL (1988). Age-related macular degeneration. Surv Ophthalmol 32, 375–413.

Bulaj G, Goldenberg DP (1999). Early events in the disulfide-coupled folding of BPTI. Protein Sci 8, 1825–1842.

Chang JY, Li L, Lai PH (2001). A major kinetic trap for the oxidative folding of human epidermal growth factor. J Biol Chem 276, 4845–4852.

Chang JY, Schindler P, Ramseier U, Lai PH (1995). The disulfide folding pathway of human epidermal growth factor. J Biol Chem 270, 9207–9216.

Cohen E *et al.* (2009). Reduced IGF-1 signaling delays age-associated proteotoxicity in mice. Cell 139, 1157–1169.

Crimmins DL, Mische SM, Denslow ND (2005). Chemical cleavage of proteins in solution. Curr Protoc Protein Sci Chapter 11, Unit 11.14.

de Jong PT (2006). Age-related macular degeneration. N Engl J Med 355, 1474–1485.

Denning GM, Anderson MP, Amara JF, Marshall J, Smith AE, Welsh MJ (1992). Processing of mutant cystic fibrosis transmembrane conductance regulator is temperature-sensitive. Nature 358, 761–764.

Evans CG, Chang L, Gestwicki JE (2010). Heat shock protein 70 (hsp70) as an emerging drug target. J Med Chem 53, 4585–4602.

Ferre F, Clote P (2005). DiANNA: a web server for disulfide connectivity prediction. Nucleic Acids Res 33, W230–W232.

Fomenko DE, Gladyshev VN (2002). CxxS: fold-independent redox motif revealed by genome-wide searches for thiol/disulfide oxidoreductase function. Protein Sci 11, 2285–2296.

Fomenko DE, Gladyshev VN (2003). Identity and functions of CxxC-derived motifs. Biochemistry 42, 11214–11225.

Fu L, Garland D, Yang Z, Shukla D, Rajendran A, Pearson E, Stone EM, Zhang K, Pierce EA (2007). The R345W mutation in EFEMP1 is pathogenic and causes AMD-like deposits in mice. Hum Mol Genet 16, 2411–2422.

Fujita J (1999). Cold shock response in mammalian cells. J Mol Microbiol Biotechnol 1, 243–255.

Hutt DM *et al.* (2010). Reduced histone deacetylase 7 activity restores function to misfolded CFTR in cystic fibrosis. Nat Chem Biol 6, 25–33.
Jager RD, Mieler WF, Miller JW (2008). Age-related macular degeneration. N Engl J Med 358, 2606–2617.
Jessop CE, Chakravarthi S, Garbi N, Hammerling GJ, Lovell S, Bulleid NJ (2007). ERp57 is essential for efficient folding of glycoproteins sharing common structural domains. EMBO J 26, 28–40.
Kostka G, Giltay R, Bloch W, Addicks K, Timpl R, Fassler R, Chu ML (2001). Perinatal lethality and endothelial cell abnormalities in several vessel compartments of fibulin-1-deficient mice. Mol Cell Biol 21, 7025–7034.
Kulka RG, Raboy B, Schuster R, Parag HA, Diamond G, Ciechanover A, Marcus M (1988). A Chinese hamster cell cycle mutant arrested at G2 phase has a temperature-sensitive ubiquitin-activating enzyme, E1. J Biol Chem 263, 15726–15731.
Kundzewicz A, Munier F, Matter JM (2008). Expression and cell compartmentalization of EFEMP1, a protein associated with malattia leventinese. Adv Exp Med Biol 613, 277–281.
Marmorstein L (2004). Association of EFEMP1 with malattia leventinese and age-related macular degeneration: a mini-review. Ophthalmic Genet 25, 219–226.
Marmorstein LY, McLaughlin PJ, Peachey NS, Sasaki T, Marmorstein AD (2007). Formation and progression of sub-retinal pigment epithelium deposits in Efemp1 mutation knock-in mice: a model for the early pathogenic course of macular degeneration. Hum Mol Genet 16, 2423–2432.
Marmorstein LY, Munier FL, Arsenijevic Y, Schorderet DF, McLaughlin PJ, Chung D, Traboulsi E, Marmorstein AD (2002). Aberrant accumulation of EFEMP1 underlies drusen formation in malattia leventinese and age-related macular degeneration. Proc Natl Acad Sci USA 99, 13067–13072.
McCracken AA, Werner ED, Brodsky JL (1998). Endoplasmic reticulum-associated protein degradation: an unconventional route to a familiar fate. Adv Mol Cell Biol 27, 165–200.
McLaughlin PJ, Bakall B, Choi J, Liu Z, Sasaki T, Davis EC, Marmorstein AD, Marmorstein LY (2007). Lack of fibulin-3 causes early aging and herniation, but not macular degeneration in mice. Hum Mol Genet 16, 3059–3070.
McLaughlin PJ *et al.* (2006). Targeted disruption of fibulin-4 abolishes elastogenesis and causes perinatal lethality in mice. Mol Cell Biol 26, 1700–1709.
Michalovitz D, Halevy O, Oren M (1990). Conditional inhibition of transformation and of cell proliferation by a temperature-sensitive mutant of p53. Cell 62, 671–680.
Mu TW, Ong DS, Wang YJ, Balch WE, Yates JR 3rd, Segatori L, Kelly JW (2008). Chemical and biological approaches synergize to ameliorate protein-folding diseases. Cell 134, 769–781.
Mullins RF, Olvera MA, Clark AF, Stone EM (2007). Fibulin-5 distribution in human eyes: relevance to age-related macular degeneration. Exp Eye Res 84, 378–380.
Piguet B, Haimovici R, Bird AC (1995). Dominantly inherited drusen represent more than one disorder: a historical review. Eye 9, 34–41.
Ringer AL, Senenko A, Sherrill CD (2007). Models of S/pi interactions in protein structures: comparison of the H2S benzene complex with PDB data. Protein Sci 16, 2216–2223.
Ron D, Walter P (2007). Signal integration in the endoplasmic reticulum unfolded protein response. Nature Rev 8, 519–529.
Roybal CN, Marmorstein LY, Vander Jagt DL, Abcouwer SF (2005). Aberrant accumulation of fibulin-3 in the endoplasmic reticulum leads to activation of the unfolded protein response and VEGF expression. Invest Ophthalmol Vis Sci 46, 3973–3979.
Schultz DW *et al.* (2003). Analysis of the ARMD1 locus: evidence that a mutation in HEMICENTIN-1 is associated with age-related macular degeneration in a large family. Hum Mol Genet 12, 3315–3323.
Sevier CS, Kaiser CA (2002). Formation and transfer of disulphide bonds in living cells. Nat Rev Mol Cell Biol 3, 836–847.
Sevier CS, Qu H, Heldman N, Gross E, Fass D, Kaiser CA (2007). Modulation of cellular disulfide-bond formation and the ER redox environment by feedback regulation of Ero1. Cell 129, 333–344.
Siegel MR, Sisler HD (1963). Inhibition of protein synthesis in vitro by cycloheximide. Nature 200, 675–676.
Sifers RN (2010). Manipulating proteostasis. Nat Chem Biol 6, 400–401.
Stone EM *et al.* (1999). A single EFEMP1 mutation associated with both malattia leventinese and Doyne honeycomb retinal dystrophy. Nat Genet 22, 199–202.
Stone EM, Sheffield VC, Hageman GS (2001). Molecular genetics of age-related macular degeneration. Hum Mol Genet 10, 2285–2292.
Tabas I, Ron D (2011). Integrating the mechanisms of apoptosis induced by endoplasmic reticulum stress. Nat Cell Biol 13, 184–190.
Tannous BA, Kim DE, Fernandez JL, Weissleder R, Breakefield XO (2005). Codon-optimized *Gaussia* luciferase cDNA for mammalian gene expression in culture and in vivo. Mol Ther 11, 435–443.
Tielsch JM, Javitt JC, Coleman A, Katz J, Sommer A (1995). The prevalence of blindness and visual impairment among nursing home residents in Baltimore. N Engl J Med 332, 1205–1209.
Timpl R, Sasaki T, Kostka G, Chu ML (2003). Fibulins: a versatile family of extracellular matrix proteins. Nature Rev 4, 479–489.
Underhill MF, Smales CM (2007). The cold-shock response in mammalian cells: investigating the HeLa cell cold-shock proteome. Cytotechnology 53, 47–53.
Usui K, Hulleman JD, Paulsson JF, Siegel SJ, Powers ET, Kelly JW (2009). Site-specific modification of Alzheimer's peptides by cholesterol oxidation products enhances aggregation energetics and neurotoxicity. Proc Natl Acad Sci USA 106, 18563–18568.
Waldo GS, Standish BM, Berendzen J, Terwilliger TC (1999). Rapid protein-folding assay using green fluorescent protein. Nat Biotechnol 17, 691–695.
Wang X, Koulov AV, Kellner WA, Riordan JR, Balch WE (2008). Chemical and biological folding contribute to temperature-sensitive DeltaF508 CFTR trafficking. Traffic 9, 1878–1893.
Werner ED, Brodsky JL, McCracken AA (1996). Proteasome-dependent endoplasmic reticulum-associated protein degradation: an unconventional route to a familiar fate. Proc Natl Acad Sci USA 93, 13797–13801.
Williamson MP (1994). The structure and function of proline-rich regions in proteins. Biochem J 297, 249–260.
Young RW (1987). Pathophysiology of age-related macular degeneration. Surv Ophthalmol 31, 291–306.
Zhang Y, Marmorstein LY (2009). Focus on molecules: fibulin-3 (EFEMP1). Exp Eye Res 90, 374–375.